Draft version August 9, 2021
Typeset using LaTeX **twocolumn** style in AASTeX63

Search for Laser Emission Lines with the Automated Planet Finder

Zoe Ko[1] and Howard Isaacson[1]

[1] *Department of Astronomy, 501 Campbell Hall, University of California, Berkeley, CA 94720-3411, USA*

ABSTRACT

We conduct a search of 852 stars for laser emission lines that are potential candidates for extraterrestrial communication. Using data obtained from the Automated Planet Finder (APF), a 2.4 meter telescope at the Lick Observatory, we search for emission lines that rise above the rest of the data, are Gaussian-shape, and are wider than the PSF of the APF. We test our algorithm and determine sensitivity by injecting 12,000 artificial signals with varying intensities and widths into 2,000 spectra. We then run the algorithm on the 5,668 spectra we have from the APF to identify potential laser line candidates.

Keywords: SETI, optical SETI, laser emission lines

1. INTRODUCTION

Traditional SETI has been primarily conducted in the radio wavelengths, with radio telescopes such as the Allen Telescope Array and the Greenbank telescope (Harp et al. 2016). However, optical lasers are promising interstellar communication tools, as they offer both privacy and high intensity. Limited diffraction prevents the signal from being observed in locations other than its intended destination, and the high intensities allow lasers to travel far distances while outshining their parent star (Tellis & Marcy 2015, 2017). Therefore, it is worthwhile to consider these shorter wavelengths as a form of extraterrestrial communication. We search through stellar spectra from the APF to find laser signals that could be potential candidates, narrowing the pool of detections down to signals with no astrophysical explanation.

2. DATA

2.1. *Targets*

We search through the spectra of 852 stars that make up a subcategory of the target selection for the Breakthrough Listen search for extraterrestrial intelligence (Isaacson et al. 2017). The entire pool of targets includes stars within 5.1 pc of the Sun, stars from the Hipparcos catalog of all spectral types along the main sequence, and nearby galaxies. The targets covered by the APF include the 5 pc and 5-50 pc spectral type complete sample (Isaacson et al. 2017). Only targets brighter than V = 12.0 are observed to ensure sufficient signal to noise ratios, and stars observed by Kick/HIRES are excluded. The APF targets include many rapidly rotating young stars that have temperatures higher than 6200 K.

Corresponding author: Zoe Ko
zko@berkeley.edu

2.2. *Observation Program*

The Automated Planet Finder covers wavelengths between 374 to 950 nm and has a high resolution of 95,000 over this region (Radovan et al. 2014). Observations for this program are taken 36 nights per year with a decker size of 10 x 30 (Isaacson et al. 2017).

2.3. *Data Reduction*

We receive APF data in the form of 1-D spectra. This data is reduced by Anna Zuckerman, who removes the echelle blaze function, normalizes the data, and Doppler shifts the spectrum. All the spectra are shifted to match the NSO solar spectrum (Yee et al. 2017).

3. METHODS

3.1. *Laser Detection Algorithm Overview*

We set the following criteria for the laser emission lines: they must exceed the noise of the data, they must be Gaussian-shaped, and they must have a FWHM greater than the PSF of the APF. The first requirement allows us to differentiate signal from noise, and we do this by finding all the pixels that are above a certain threshold. The threshold is defined as $T = n \cdot m$, where m is the median flux value of all the lines above the continuum level, and n is an arbitrary value that maximizes detection and minimizes false positives. The signals must be Gaussian-shaped to indicate that they were

smeared out by the telescope resolution and therefore actually passed through the telescope. To confirm this, we fit a Gaussian to each signal that exceeds the threshold and run a chi-squared test that measures how closely the signal fits the Gaussian. If chi-squared is under 11, the signal is categorized as Gaussian-like and moves on to the final test. The signal FWHM must be wider than 2.7 pixels, which is the PSF of the APF; anything narrower is indicative of a cosmic ray hit or a systematic error. If a detection passes all three of these tests, it moves onto the next step in verifying it as an extraterrestrial laser emission line.

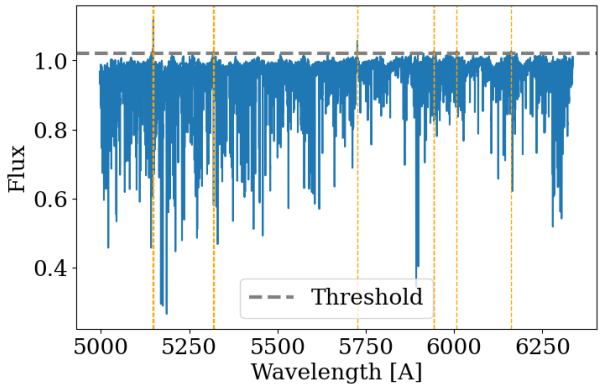

Figure 1: Given an APF spectrum, we first identify all pixels that rise above the established threshold.

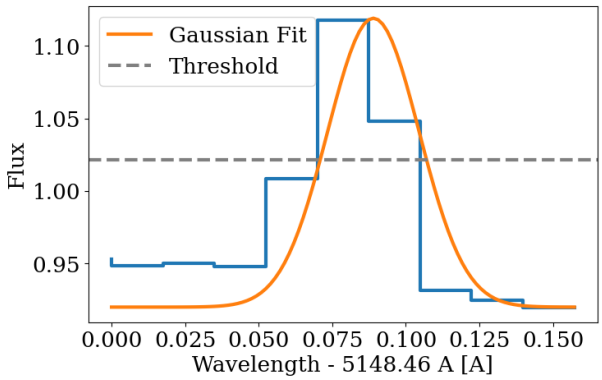

Figure 2: We then iterate through every signal that exceeds the threshold and test if it is Gaussian-like with a FWHM greater than 2.7 pixels.

3.2. *Testing the Algorithm: Signal Injection and Recovery*

We tested the algorithm by running it on spectra with artificially injected signals. We took 2,000 random spectra from our APF data and injected 6 random Gaussians into each spectra, which had heights ranging from 0.1 to 0.3 in flux and widths from 1 to 12 pixels. We used a threshold of $T = m + 1.05$, where we arbitrarily set the n value to 1.05. For signals wider than the PSF of the APF and above the established threshold, we obtained a recovery rate of 100%. For all signals below the established threshold, we obtained a 0% recovery rate, as expected. For signals narrower than the PSF and higher than the established threshold, we obtained a recovery rate of 30%. This is because the width of each signal is estimated by fitting a Gaussian to it and calculating the FWHM. Therefore, some signals that are narrower than the PSF are recovered because the detection algorithm overestimates their widths.

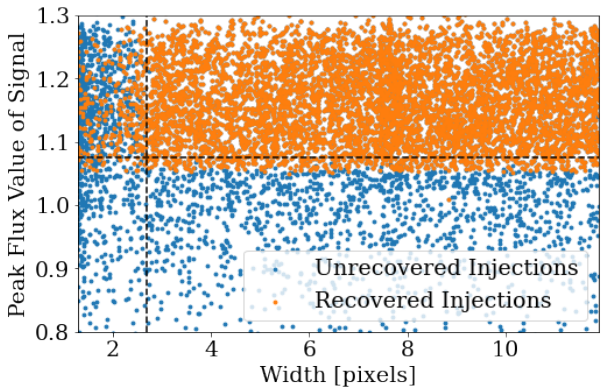

Figure 3: All points to the right of the dashed vertical line represent signals wider than the PSF. All points above the dashed horizontal line represent signals with flux values above the maximum threshold value.

3.3. *Determining the Threshold*

The threshold is defined as $T = n \cdot m$, where m is the median flux value of all the lines above the continuum level, and n is an arbitrary value that maximizes detection and minimizes false positives. We initially set n to be 1.05 arbitrarily and ran the detection algorithm on all the data. However, we found that low SNR targets received a high number of detections while high SNR targets received a low number of detections, which can be seen in figure 4. Because there is no astrophysical reason as to why SNR would affect the number of emission lines in a spectrum, we concluded that noise caused the difference in number of detections. We decided to allow n to vary across spectra, depending on the SNR. For spectra with SNR above 150, we increased the sensitivity of our algorithm, using an n value of 1.02. For spectra with SNR below 10, we decreased the sensitivity of our algorithm, using an n value of 1.13. For the remaining spectra, we used an n value of 1.05.

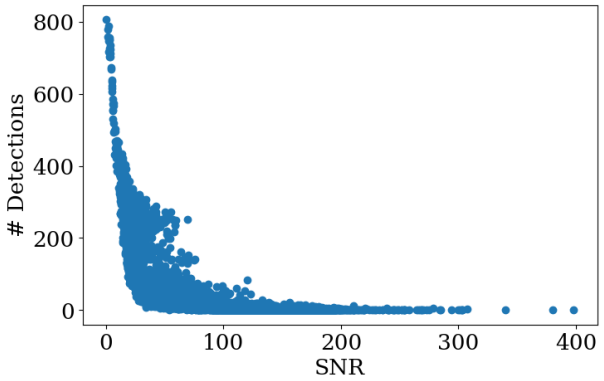

Figure 4: The relationship between SNR and number of detections across the spectra.

4. RESULTS

We ran the algorithm on our APF data, allowing n to vary across the spectra, depending on the SNR. We searched through 5,868 spectra, which corresponds to 852 unique stars. For each star, we calculated the median number of detections across all its spectra. We obtained 249,066 detections across all of our spectra.

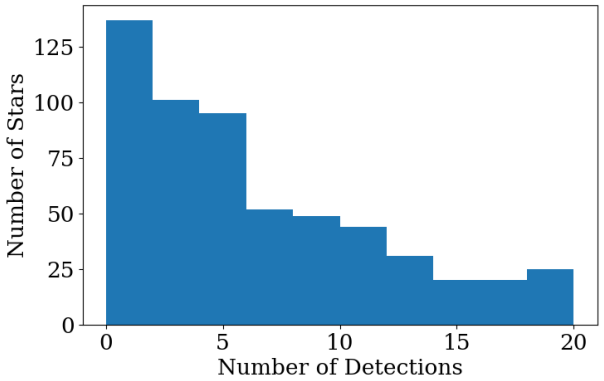

Figure 5: 67% of the stars have under 20 detections.

We inspected detections from high SNR targets with few detections by eye to better understand the nature of the detections our algorithm marks.

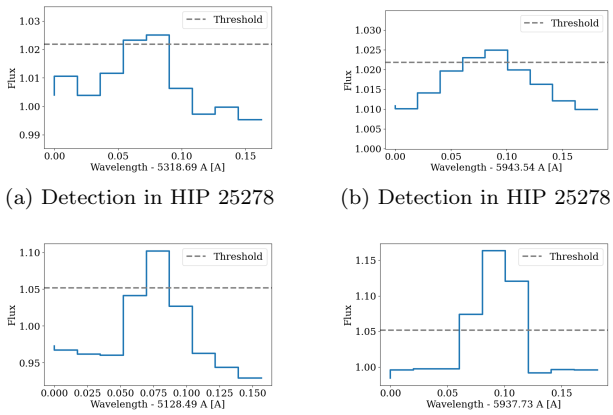

(a) Detection in HIP 25278 (b) Detection in HIP 25278

(c) Detection in HIP 85829 (d) Detection in HIP 85829

Figure 6: Examples of potential laser line candidates marked by our detection algorithm.

5. DISCUSSION

Although we allowed n to vary, depending on SNR, there is still a correlation between number of detections and SNR, which stems from our parameters rather than from an astrophysical reason.

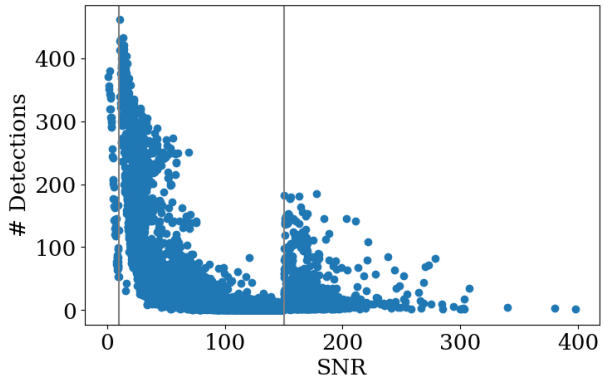

Figure 7: By allowing n to vary across different spectra with different SNRs, the number of detections is lowered for noisy data and increased for clean data. However, there is still a correlation.

Therefore, a future implementation could allow n to vary as a function of SNR, or we could establish a unique threshold for each spectrum such that 10% of its pixels exceeds the threshold. This would create a uniform number of detections across all spectra. Creating this uniformity is valid because we have no priors on the relationship between number of detections and SNR or other stellar parameters.

Next steps also include further identifying characteristics that distinguish laser lines from astrophysical

sources and categorizing each of our detections, narrowing down the candidates to detections from unknown sources.

6. CONCLUSION

We successfully developed a laser detection algorithm that is sensitive to all signals wider than the PSF of the APF and with flux values higher than $T = m * n$, where m is the median flux value of all the lines above the continuum level, and n is either 1.02, 1.05, or 1.13, depending on the SNR of the spectrum. After running this detection algorithm on our APF data, we obtained 249,066 total detections. We will begin to classify each detection into categories that include cosmic ray hits, night sky emission lines, and stellar emission lines. The APF spectra offer an abundance of data that may contain laser emission lines from extraterrestrial intelligence, and we plan to categorize each detection until we obtain a pool of candidates that have no astrophysical or terrestrial source.

ACKNOWLEDGMENTS

This work was supported by the Berkeley SETI Research Center under the supervision of Howard Isaacson and Steve Croft.

REFERENCES

Harp, G., Richards, J., Shostak, S., et al. 2016, The Astrophysical Journal, 825, 155

Isaacson, H., Siemion, A. P., Marcy, G. W., et al. 2017, Publications of the Astronomical Society of the Pacific, 129, 054501

Radovan, M. V., Lanclos, K., Holden, B. P., et al. 2014, in Ground-based and Airborne Telescopes V, Vol. 9145, International Society for Optics and Photonics, 91452B

Tellis, N. K., & Marcy, G. W. 2015, Publications of the Astronomical Society of the Pacific, 127, 540

—. 2017, The Astronomical Journal, 153, 251

Yee, S. W., Petigura, E. A., & Von Braun, K. 2017, The Astrophysical Journal, 836, 77